C1*s* and O1*s* photoelectron satellite spectra of CO with symmetry-dependent vibrational excitations

M. Ehara,[a] K. Kuramoto,[b] and H. Nakatsuji[c]
Department of Synthetic Chemistry and Biological Chemistry, Graduate School of Engineering, Kyoto University, Kyoto 615-8510, Japan

M. Hoshino, T. Tanaka, M. Kitajima,[d] and H. Tanaka
Department of Physics, Sophia University, Chiyoda-ku, Tokyo 102-8554, Japan

A. De Fanis and Y. Tamenori
SPring-8/JASRI, Sayou-gun, Hyogo 679-5198, Japan

K. Ueda[e]
Institute of Multidisciplinary Research for Advanced Materials, Tohoku University, Sendai 980-8577, Japan

(Received 13 June 2006; accepted 7 August 2006; published online 18 September 2006)

The photoelectron shake-up satellite spectra that accompany the C1*s* and O1*s* main lines of carbon monoxide have been studied by a combination of high-resolution x-ray photoelectron spectroscopy and accurate *ab initio* calculations. The symmetry-adapted cluster-expansion configuration-interaction general-*R* method satisfactorily reproduces the satellite spectra over a wide energy region, and the quantitative assignments are proposed for the 16 and 12 satellite bands for C1*s* and O1*s* spectra, respectively. Satellite peaks above the $\pi^{-1}\pi^{*}$ transitions are mainly assigned to the Rydberg excitations accompanying the inner-shell ionization. Many shake-up states, which interact strongly with three-electron processes such as $\pi^{-2}\pi^{*2}$ and $n^{-2}\pi^{*2}$, are calculated in the low-energy region, while the continuous Rydberg excitations are obtained with small intensities in the higher-energy region. The vibrational structures of low-lying shake-up states have been examined for both C1*s* and O1*s* ionizations. The vibrational structures appear in the low-lying C1*s* satellite states, and the symmetry-dependent angular distributions for the satellite emission have enabled the Σ and Π symmetries to be resolved. On the other hand, the potential curves of the low-lying O1*s* shake-up states are predicted to be weakly bound or repulsive. © *2006 American Institute of Physics*. [DOI: 10.1063/1.2346683]

I. INTRODUCTION

Shake-up satellites that appear in the photoelectron spectra are challenging spectroscopic subjects from both theoretical and experimental viewpoints. Theoretically, a precise description of the satellite states is possible only with advanced theoretical methods because the spectra reflect very complex electron-correlation and orbital-reorganization effects.[1] Experimentally, the weak intensities of photoelectron satellites make high-resolution photoelectron spectroscopy difficult.

Recently, scientists have had a renewed interest in studies of the inner-shell photoelectron satellites because significant developments in both high-resolution x-ray photoelectron spectroscopy (XPS) and accurate theoretical methods have allowed precise knowledge and assignments of the inner-shell satellite spectra to be obtained. A high photon flux with very narrow photon bandwidths, which are available using high-resolution soft x-ray monochromators installed at high-brilliance third-generation synchrotron radiation light sources,[2] has opened the new possibility of detailed spectroscopy for the geometry relaxation in core-electronic states.[3] Vibrational structures, which allow the stable geometry of the states to be discussed, can be observed in a core-level photoelectron satellite spectrum. This situation has further motivated intensive cooperative research from experimental and theoretical sides, on the shake-up states associated with the inner-shell ionization.

The inner-shell photoelectron satellite spectra of molecules were measured extensively around 1970.[4,5] Schirmer *et al.* observed the first detailed inner-shell satellite spectra of CO in the energy region up to ~80 and ~60 eV for the C1*s* and O1*s* main lines, respectively.[6] Nordfors *et al.* measured the O1*s* satellite spectrum up to ~50 eV relative to the O1*s* ionization.[7] However, the resolution of the spectra in the 1980's is insufficient to examine the detailed peak structure, especially in the high energy region. Theoretically, calculating the shake-up satellite spectra of CO has been challenging, in particular, it has been difficult to obtain an accurate relative energy for $\pi-\pi^{*}$ transitions. Guest *et al.* performed the configuration interaction calculations for the first five $^{2}\Sigma^{+}$ C1*s* core-hole states.[8] Angonoa *et al.* used the algebraic

[a]Also at Fukui Institute for Fundamental Chemistry, Kyoto University, Kyoto 606-8103, Japan. Electronic mail: ehara@sbchem.kyoto-u.ac.jp
[b]Present address: Toyota Central R&D Labs, Inc., Nagakute, Aichi 480-1192, Japan
[c]Electronic mail: hiroshi@sbchem.kyoto-u.ac.jp
[d]Present address: Department of Chemistry, Tokyo Institute of Technology, Tokyo 152-8551, Japan.
[e]Electronic mail: ueda@tagen.tohoku.ac.jp

diagrammatic construction (ADC) method to calculate the satellite spectra up to ~22 and ~24 eV for C1*s* and O1*s* ionizations, respectively.[9] They also studied the low-lying satellite states of Π, Δ, and Σ^- symmetries. However, these theoretical works addressed only the valence excitations in the low-energy region; Rydberg transitions were not examined. Fronzoni *et al.* reported the important theoretical assignments for both the C1*s* and O1*s* satellite spectra of CO using the quasidegenerate perturbation theory within the configuration interaction (QDPTCI) method.[10] Recently, Thiel *et al.* performed the fourth order ADC calculations.[11] In addition, the dynamics of the conjugate satellites were also studied in detail.[12] The QDPTCI results seem to be the most reliable assignments of the satellite spectra over a wide energy region. However, there are still discrepancies in some points between the theoretical results and the experimental spectra. Thus, further intensive cooperative investigations by high-resolution XPS and an accurate theoretical method are necessary to elucidate the fine details of the shake-up satellite spectra that accompany the C1*s* and O1*s* main lines of CO.

Recently, we have investigated the vibrationally resolved C1*s* and O1*s* main lines of CO (Ref. 13) and the N1*s* main line of N_2 (Ref. 14) both experimentally and theoretically. The potential curves of the inner-shell single-hole states were extracted from the experimentally determined vibrational intensity ratios on the basis of a Franck-Condon (FC) analysis. The vibrational spectra were well reproduced by *ab initio* calculations based on the symmetry-adapted cluster-expansion configuration-interaction (SAC-CI) method.[15] Furthermore, we observed vibrationally resolved photoelectron satellite bands due to the N1*s* photoionization in N_2 (Ref. 15) where the two-hole one-electron (satellite) states of the Σ and Π symmetries were resolved using an angle-resolved technique. *Ab initio* calculations based on the SAC-CI method well reproduced the vibrational excitation of the observed satellite bands. The gerade and ungerade splittings of the shake-up satellite states were calculated to be quite small compared to the main line.

In the present work, the inner-shell satellite spectra of CO are measured by the high-resolution XPS and analyzed in detail by the SAC/SAC-CI method.[15] The vibrational levels of the low-lying C1*s* satellite states are also investigated with the angle-resolved measurements and accurate potential energy curves, as briefly illustrated in our preliminary report.[16] In the present paper, we also discuss the vibrational levels of the O1*s* satellite states. The theoretical method applied here is the SAC-CI general-*R* method,[17] which has been designed to accurately describe multiple-electron processes. This method is useful for studying the satellite peaks which appear in both the valence[18] and inner-shell[19–22] ionization spectra. Recently, we have successfully applied this method to the various types of core-level spectroscopy studies; the core electron binding energies (CEBEs) of molecules,[19] the vibrational spectrum of H_2O,[20] and the satellite spectra of CH_4, NH_3,[19] H_2O,[21] and formaldehyde.[22] This paper clearly shows that the satellite spectra of CO are more characteristic and complex than these molecules.

II. EXPERIMENT

The experiments were conducted at the *c* branch of the soft x-ray photochemistry beamline 27SU (Ref. 23) at SPring-8, the 8 GeV synchrotron radiation facilities in Japan. The monochromator installed in this beam line is a Hettrick type with a high resolution between 10 000 and 20 000.[24] Another notable feature of the beamline is a figure 8 undulator[25] as the light source, which enables angle-resolved electron spectroscopic measurements. This undulator can switch the direction of the polarization vector from horizontal to vertical and vice versa solely by varying the gap of the undulator. Measuring the 2*s* and 2*p* photoelectrons of Ne confirmed that the degree of light polarization was better than 0.98 for both directions. The electron spectroscopy apparatus installed on the beamline consists of a hemispherical electron analyzer (Gamadata-Scienta SES-2002) with a Herzog-plate termination and accelerating-retarding multielement, a gas cell, and a differentially pumped chamber.[26] A combination of this electron spectroscopy apparatus and the state-of-the-art soft x-ray beamline provides an excellent opportunity to perform high-resolution XPS.[24,27]

The CO target gas was introduced into the gas cell during the measurements. The background pressure of $\sim 10^{-4}$ Pa was measured in the experimental chamber where the gas cell was placed. The wide-range C1*s* and O1*s* photoelectron satellite spectra of CO were recorded at photon energies 400 and 650 eV, respectively, with overall experimental resolutions of $\Delta E = 160$ meV using the horizontal polarization. In addition, the C1*s* low-energy satellite bands were recorded at two photon energies 310 and 330 eV, with $\Delta E = 100$ meV using both the horizontal and vertical polarizations. The O1*s* low-energy satellite bands were recorded at similar high resolutions. However, we have not identified any vibrational structures and the spectrum looks nearly identical to the one recorded at lower resolution. Thus, the data is not presented.

III. COMPUTATIONAL DETAILS

To assign the satellite spectra over a wide energy region, the vertical core-electron ionization spectra were calculated with the R_{CO} fixed to the experimental value of 1.1283 Å.[28] We used extensive basis sets to describe the orbital reorganization and electron correlations so that the quality was similar to our study on H_2CO;[22] i.e., triple zeta (VTZ) $(10s6p)/[6s3p]$ GTOs for C and O (Ref. 29) augmented with two polarization *d* functions[30] and Dunning's Rydberg functions $[2s2p2d]$.[31] The resultant basis sets were $(12s14p4d)/[8s8p4d]$ and the number of atomic orbitals (AOs) was 104.

To analyze the vibrational spectra of the low-lying C1*s* and O1*s* shake-up satellite states, we conducted the *ab initio* calculations of the potential energy curves for the ground state and the $^2\Sigma^+$, $^2\Pi$, $^2\Delta$, and $^2\Sigma^-$ satellite states in the region of $R = 0.9–1.7$ Å. Extensive basis sets of triple zeta (VTZ) $(10s6p)/[5s3p]$ GTOs of the group of Schaefer *et al.*[29] with two polarization *d* functions were adopted; the transition to the Rydberg states were well separated from these states.

TABLE I. Dimensions of the selected SAC-CI general-*R* operators for the vertical *K*-shell ionizations of CO.

	Singles	Doubles	Triples	Quadruples	Total
C1*s*	5	225	18 640	88 028	106 898
O1*s*	5	225	19 313	90 042	109 585

We used the SAC-CI general-*R* method to describe the C1*s* and O1*s* core ionization and the shake-up satellite spectra. The reference functions were closed-shell Hartree-Fock orbitals; core-localized orbitals were not adopted. We used different sets of *R* operators for the C1*s* and O1*s* ionizations. We investigated the satellites dominantly described by doubles with a considerable contribution of triples. Hence, we included the *R* operators up to quadruples in the general-*R* calculation. To describe core-hole relaxation, all the molecular orbitals (MOs) were included in the active space.

To reduce the computational requirements, the perturbation selection procedure was adopted.[32] Reference functions for perturbation selection were due to the small-active-space SDT-CI vectors to ensure the accuracy up to at least three-electron processes; this is important for the general-*R* calculations of the inner-shell satellite spectra. The threshold of the linked terms for the ground state was set at $\lambda_g = 1.0 \times 10^{-6}$ a.u., and the unlinked terms were adopted as the products of the important linked terms with SDCI coefficients larger than 0.005. For the inner-shell ionized states, the thresholds of the linked terms, which are doubles and triples, were set at $\lambda_e = 1.0 \times 10^{-7}$, and those of the quadruples were set at 1.0×10^{-6}. To calculate the potential energy curves, the threshold of quadruples was also set to $\lambda_e = 1.0 \times 10^{-7}$. The thresholds of the CI coefficients used to calculate the unlinked operators in the SAC-CI method were 0.05 and 0.001 for the *R* and *S* operators, respectively. Table I summarizes the dimensions of the selected SAC-CI linked operators employed for the vertical ionization spectra.

The ionization cross sections were calculated using the monopole approximation[33] to estimate the relative intensities of the peaks. Both the initial- and final-ionic-state correlation effects were included.

The calculated potential energy curves were fitted with the extended Rydberg functions, and the vibrational analysis was performed. To simulate the photoelectron spectrum, vibrational wave functions and Franck-Condon factors were obtained using the grid method in which the Lanczos algorithm was adapted for the diagonalization.

The SAC/SAC-CI calculations were executed with the GAUSSIAN03 suite of programs[34] with some modifications to calculate the inner-shell ionization spectra; namely, the reference SDT-CI was enabled in the SAC-CI calculation. The vibrational analysis was performed with the MCTDH program package.[35]

IV. RESULTS AND DISCUSSION

A. C1*s* satellite spectrum

First, we have investigated the vertical C1*s* shake-up satellite spectrum over a wide energy region. Figure 1 presents the SAC-CI general-*R* spectrum along with the measured XPS spectrum. In the theoretical spectrum, the calculated pole strengths are shown by solid vertical lines and are convoluted using Gaussians with the full widths at half maximum (FWHMs) of 0.5 eV. Table II summarizes the ionization potentials with the relative energies to the main line, relative monopole intensities, and SAC-CI main configurations for the C1*s* shake-up satellite states of CO. Only states with relative intensities larger than 0.0005 are listed. Many other states with negligible intensities are not given. The CEBE of the C1*s* main line is calculated to be 296.13 eV, which is consistent with the recent experimental adiabatic ionization potential (IP) of 296.069 eV.[36] The present XPS measurement gives a high-resolution spectrum, which contains fine peak structures in some bands due to the vibrational progression and/or numerous satellite states. Our present analysis has identified 16 satellite bands in the energy region of 0–30 eV.

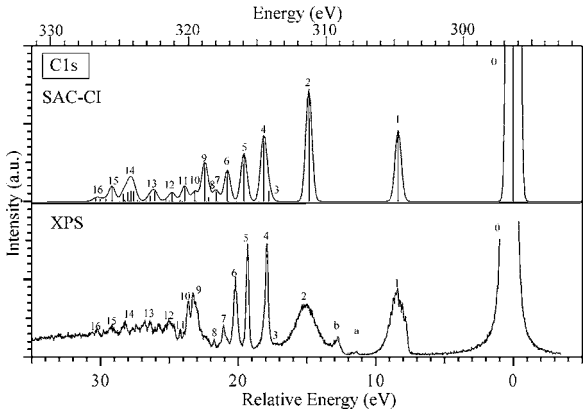

FIG. 1. C1*s* photoelectron satellite spectrum of CO. The experimental spectrum is recorded at a photon energy of 400 eV.

As seen from Fig. 1, the theoretical spectrum satisfactorily reproduces the shape of the experimental satellite spectrum, although the intensity of the XPS does not necessarily agree with the theoretical monopole intensity. Satellite band 1 was assigned to the pure $\pi^{-1}\pi^*$ shake-up state.[8–10] This assignment has also been confirmed in the present calculation; the calculated energy of this state is 8.38 eV, and the observed value is 8.43 eV. The calculated relative intensity is 0.0218, while the experimental values are between 0.025 (this work) and 0.023.[6] As discussed later, a detailed C–O vibrational analysis of this state is also performed in this energy region using XPS and SAC-CI with two $^2\Pi$ states of $\pi^{-1}\pi^*$ transitions. The small structures labeled as *a* and *b* are assigned to conjugate satellites and no satellite states with Σ^+ symmetry are calculated in this energy region.

The experimental intensity should be considered when comparing to the theoretical intensity. We chose photon energies that are approximately 100 eV above the threshold. Although this is not near threshold, the cross sections may have not yet become stationary at this energy. The experimental intensities roughly agree with the earlier study of Schirmer *et al.*, which was conducted at a much higher energy,[6] but are not identical. These minor discrepancies may indicate the dynamics of the satellite branching ratios.

TABLE II. Ionization energy (eV), relative energy to the main line (ΔE, eV), monopole intensity, and main configurations of the C1*s* satellite states of CO.

Other works					This work						
Expt.[a]		ADC(4)[b]		QDPTCI[c]	Expt.		SAC-CI general *R*				
ΔE	Int.	ΔE	Int.	ΔE	ΔE	Int.	No.	IP	ΔE	Int.	Main configurations ($\|C\|>0.25$)
296.069[d]	1	296.08	1	295.46	0.00	1	0	296.13	0.00	1	$0.81(2\sigma^{-1})+0.22(\pi^{-1}\pi^{*}2\sigma^{-1})+0.22(\pi^{-1}\pi*2\sigma^{-1})$
8.34	0.023	9.11	0.022	8.61	8.43	0.025	1	304.51	8.38	0.0218	$0.67(2\sigma^{-1}\pi^{*}\pi^{-1})+0.67(2\sigma^{-1}\pi^{*}\pi^{-1})$ $+0.33(\pi^{-1}\pi^{*}2\sigma^{-1})+0.33(\pi^{-1}\pi^{*}2\sigma^{-1})$
14.88	0.048	17.12	0.050	15.42	15.05	0.039	2	311.00	14.87	0.0336	$0.35(\pi^{-1}\pi^{*}2\sigma^{-1})+0.35(\pi^{-1}\pi^{*}2\sigma^{-1})-0.35(\pi^{-1}\pi^{*}\pi^{-1}\pi^{*}2\sigma^{-1})$
				17.37			3	313.92	17.79	0.0017	$0.55(5\sigma^{-1}\pi^{*}5\sigma^{-1}\pi^{*}2\sigma^{-1})+0.27(\pi^{-1}\pi^{*}2\sigma^{-1})$ $+0.27(\pi^{-1}\pi*2\sigma^{-1})$
17.85	0.019	19.89	0.013	18.06,18.46	17.93	0.016	4	314.29	18.16	0.0173	$0.55(5\sigma^{-1}6\sigma2\sigma^{-1})+0.27(\pi^{-1}\pi^{*}\pi^{-1}\pi^{*}2\sigma^{-1})$
19.22	0.011	20.79	0.004	19.50	19.33	0.012	5	315.72	19.59	0.0075	$0.36(2\sigma^{-1}6\sigma5\sigma^{-1})+0.33(2\sigma^{-1}\sigma^{*}5\sigma^{-1})$
20.09	0.016	21.18	0.002	20.57	20.20	0.009	6	316.92	20.79	0.0048	$0.35(2\sigma^{-1}9\sigma5\sigma^{-1})+0.35(4\sigma^{-1}\pi^{*}2\sigma^{-1}\pi^{*}5\sigma^{-1})$
21.1	0.004	21.64	0.017	21.32,21.82	21.10	0.004	7	317.74	21.61	0.0018	$0.37(5\sigma^{-1}9\sigma2\sigma^{-1})+0.36(5\sigma^{-1}\pi^{*}4\sigma^{-1}\pi^{*}2\sigma^{-1})$ $+0.36(5\sigma^{-1}\pi^{*}4\sigma^{-1}\pi^{*}2\sigma^{-1})$
22.2	0.005	22.31	0.007	22.14	21.75	0.002	8	318.26	22.13	0.0006	$0.34(\pi^{-1}\pi^{*}\pi^{-1}\pi^{*}2\sigma^{-1})+0.34(\pi^{-1}\pi^{*}\pi^{-1}\pi^{*}2\sigma^{-1})$ $+0.32(2\sigma^{-1}\sigma*5\sigma^{-1})$
23.2	0.027			22.73,23.05	23.30	0.011	9	318.57	22.44	0.0059	$0.41(5\sigma^{-1}\sigma^{*}2\sigma^{-1})+0.30(2\sigma^{-1}3\sigma5\sigma^{-1})$
				23.38,23.52	23.63	0.009	10	319.28	23.15	0.0016	$0.38(2\sigma^{-1}7\sigma5\sigma^{-1})+0.30(5\sigma^{-1}\sigma*2\sigma^{-1})$
				23.85,23.97			11	320.02	23.89	0.0023	$0.38(2\sigma^{-1}7\sigma5\sigma^{-1})+0.30(5\sigma^{-1}9\sigma2\sigma^{-1})$
25.8				24.93	25.00	⋯	12	320.93	24.80	0.0014	$0.41(2\sigma^{-1}8\sigma5\sigma^{-1})+0.35(5\sigma^{-1}8\sigma2\sigma^{-1})$
				25.65,25.90	26.2	⋯	13	322.20	26.07	0.0015	$0.33(2\sigma^{-1}6\sigma4\sigma^{-1})-0.30(4\sigma^{-1}6\sigma2\sigma^{-1})$ $+0.29(2\sigma^{-1}\sigma*4\sigma^{-1})$
26.6				26.16,26.22	26.7	⋯		322.54	26.41	0.0009	$0.43(5\sigma^{-1}7\sigma2\sigma^{-1})+0.39(5\sigma^{-1}11\sigma2\sigma^{-1})$ $+0.36(2\sigma^{-1}11\sigma5\sigma^{-1})$
				26.91,27.14			14	323.73	27.60	0.0016	$0.37(5\sigma^{-1}11\sigma2\sigma^{-1})+0.33(2\sigma^{-1}11\sigma5\sigma^{-1})$ $-0.27(5\sigma^{-1}9\sigma2\sigma^{-1})$
				27.33				323.93	27.80	0.0016	$0.45(5\sigma^{-1}11\sigma2\sigma^{-1})+0.42(2\sigma^{-1}11\sigma5\sigma^{-1})$ $-0.35(5\sigma^{-1}7\sigma2\sigma^{-1})$
28.2				28.15	28.1	⋯		324.14	28.01	0.0014	$0.53(5\sigma^{-1}10\sigma2\sigma^{-1})+0.45(2\sigma^{-1}10\sigma5\sigma^{-1})$
⋯								324.48	28.35	0.0011	$0.49(5\sigma^{-1}11\sigma2\sigma^{-1})+0.45(2\sigma^{-1}11\sigma5\sigma^{-1})$
29.2					29.1	⋯	15	325.30	29.17	0.0023	$0.40(\pi^{-1}3\pi2\sigma^{-1})+0.33(\pi^{-1}3\pi2\sigma^{-1})$
~32.5					30.2	⋯	16	326.17	30.04	0.0004	$0.52(2\sigma^{-1}3\pi\pi^{-1})-0.30(2\sigma^{-1}4\pi\pi^{-1})$
								326.50	30.37	0.0005	$0.44(\pi^{-1}4\pi2\sigma^{-1})+0.42(2\sigma^{-1}4\pi\pi^{-1})+0.35(2\sigma^{-1}4\pi\pi^{-1})$

[a]Reference 6.
[b]Reference 9.
[c]Reference 10.
[d]Reference 36.

The strongest band 2 has been previously assigned to the shake-up state arising from the singlet-type $\pi^{-1}\pi^{*}$ transition strongly interacting with the double excitation $\pi^{-2}\pi^{*2}$.[8–10] The present result is consistent with this assignment. It has been difficult to theoretically reproduce the relative energy of this state; the calculated relative energies were 17.06 and 15.42 eV by the ADC(4) (Ref. 9) and QDPTCI,[10] respectively, but the experimental values were 15.05 (this work) and 14.88 eV.[6] The present calculation gave 14.87 eV with a large relative intensity of 0.0336, which agrees reasonably well with the experimental value of 0.039. It is noteworthy that in the case of formaldehyde, the three-electron process $n^{-2}\pi^{*2}$ appears in a much lower energy region.[22] Similar to band 1, the fine peak structures observed for this band can be attributed to the vibrational components because there are no other satellite states in this region.

Weak satellite peak 3, which is just below sharp peaks 4–7, is calculated at 17.79 eV with a very small intensity. This peak is dominantly assigned to the double excitation, $n^{-2}\pi^{*2}$ transition. Fronzoni *et al.* obtained this state by the QDPTCI method and gave the same assignment.[10] However, their calculated pole strength was larger than the present calculation and their theoretical spectrum significantly differed from our experiment in this region.[10]

Peaks 4–7 have narrow peak shapes. Peak 4, which is observed at 17.93 eV is assigned to the $5\sigma^{-1}6\sigma(n^{-1}6\sigma)$ state, that is calculated at 18.16 eV with a relatively large intensity of 0.0173. This state has the characteristics of a $\pi^{-2}\pi^{*2}$ transition. Peaks 5–7 are observed at 19.33, 20.20, and 21.10 eV relative to the main peak. These peaks are also assigned to the $5\sigma^{-1}6\sigma$ or $5\sigma^{-1}9\sigma$ transitions that interact with the three-electron process of $4\sigma^{-1}5\sigma^{-1}\pi^{*2}(n^{-1}\pi^{-1}\pi^{*2})$.

Gelius observed a peak at 23.3 eV and assigned it to a $\pi^{-1}3p\pi$ transition.[5] Fronzoni *et al.* calculated some shake-up states in this energy region.[10] We have measured two peaks, 9 and 10, at 23.30 and 23.63 eV, respectively. The SAC-CI calculation gives $5\sigma^{-1}n\sigma$ and $5\sigma^{-1}3p$ transitions with relatively large intensities. Continuous peaks 11–16 are observed in the higher energy region of these two peaks. For these

peaks, numerous Rydberg transitions are calculated. These states are described by the linear combinations of Rydberg transitions such as $5\sigma^{-1}np$ and $5\sigma^{-1}nd$.

B. Low-lying C1*s* satellite states

Next, we examine the low-lying C1*s* shake-up satellite states in the energy region of 8–10 eV. The preliminary report is given elsewhere.[16] The photoelectron satellites provide evidence for the breakdown of the independent particle picture and are thus called correlation satellites.[1,37] The correlation satellites can be phenomenologically classified into two groups.[38] The first group includes satellites with excitation cross sections that remain nearly constant relative to the single-hole ionization cross section, while the second group includes those with excitation cross sections that sharply decrease as the energy increases. These two different types of energy dependences have been attributed to the two lowest-order correlation terms, which are often called the direct and conjugate shake-up terms.[39] The conjugate shake-up contribution is significant near the ionization threshold region and rapidly decreases as the energy increases.[37,39] The conjugate contributions become negligible at high energy due to the sharp drop in the bound-free overlap integral. At this limit, the direct shake-up satellite band mimics the mainline both in the excitation cross section and in the asymmetry parameter β of the electron emission: β approaches the limiting value of two. It should be noted that the direct and conjugate channels may have the same final state and thus interference occurs.[12]

The low-lying two-hole one-electron states concerned here have electron configurations of $2\sigma^{-1}\pi^{-1}\pi^{*}(^2\Sigma)$ and $2\sigma^{-1}5\sigma^{-1}\pi^{*}(^2\Pi)$. The transitions, which lead to the $2\sigma^{-1}\pi^{-1}\pi^{*}(^2\Sigma)$ state, are dominated by the direct shake-up term: the conjugate shake-up term also contributes at low excitation energy. The transitions, which lead to the $2\sigma^{-1}5\sigma^{-1}\pi^{*}(^2\Pi)$ state, are dominated by the conjugate shake-up contribution. Angonoa *et al.*[9] estimated the vertical ionization energy of the $^2\Sigma^+$ state to be 9.11 eV and those of $^2\Pi$ to be 8.44 and 9.20 eV. Thus the low-lying photoelectron satellite bands arising from the transitions to the $^2\Sigma^+$ and $^2\Pi$ states should overlap in energy.

Figure 2 shows the low-lying satellite bands recorded at photon energies of 310 and 330 eV at 0° and 90° relative to the polarization vector of the incident radiation. At 310 eV in the 90° spectrum, two vibrational bands are observed. However, in the 0° spectrum, peaks that are not seen in the 90° spectrum appear. When the photon energy is increased from 310 to 330 eV, the spectra change dramatically due to a rapid intensity drop of the 90° spectrum and of the same band in the 0° spectrum. These spectra clearly indicate that at least three electronic states are involved.

Based on the observed energy dependence and the angular distribution of the satellite spectra, we can decompose the contributions into the direct and conjugate terms. Using the characteristics of the direct and conjugate shake-up contributions described above, we can assign the three observed vibrational bands in Fig. 2. The band which appears in the 0° spectrum at 330 eV nearly disappears in the 90° spectrum

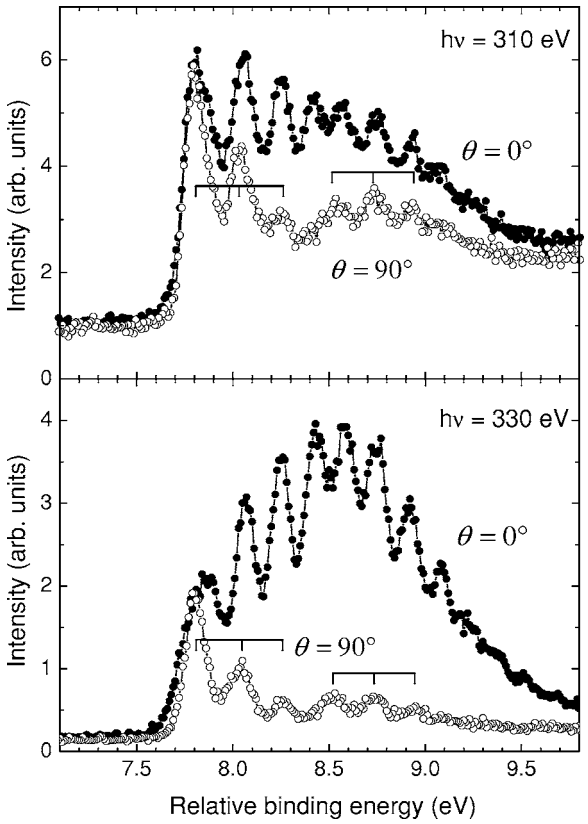

FIG. 2. The C1*s* photoelectron satellite spectra of CO recorded at photon energies of 310 eV (upper) and 330 eV (lower panel), at 0° and 90° relative to the polarization vector. The spectra are plotted as a function of the binding energy relative to the C1*s* single-hole state.

and exhibits a very strong anisotropy with β near two. Thus, it is concluded that this band is dominated by the direct shake-up contribution and is assigned to the transition to the ionic final states $2\sigma^{-1}\pi^{-1}\pi^{*}(^2\Sigma^+)$. On the other hand, the two bands, which appear in the 90° spectrum at 330 eV, are attributed to the conjugate shake-up contributions. Thus, these bands are assigned to the transitions to the $2\sigma^{-1}5\sigma^{-1}\pi^{*}(^2\Pi)$ states.

We have performed *ab initio* calculations of the relevant potential curves using the SAC-CI method. It should be noted that in the present calculations, the intensities of the $^2\Pi$, $^2\Delta$, and $^2\Sigma^-$ states are zero due to symmetry, and the intensities of the conjugate satellites cannot be evaluated. Figure 3 shows the resulting potential energy curves of the C1*s* shake-up satellite states. The overall characteristics of the potential energy curves are similar to those of N_2.[14] The geometry relaxation by the shake-up ionization of CO is large for the $^2\Sigma^+$ state and the elongation is predicted to be 0.166 Å (r_e=1.292 Å). This change is almost the same as that in N_2, 0.164 Å,[14] because the shake-up $^2\Sigma^+$ state is characterized by a $\pi-\pi^*$ transition for both molecules. The geometry relaxation for the $^2\Pi$ states is much smaller: the equilibrium distances of the lower and higher $^2\Pi$ states are r_e =1.168 and 1.194 Å, respectively. The geometry changes of these states, 0.042 and 0.068 Å, are smaller than the corresponding changes for N_2, 0.066 and 0.091 Å.[14] The differences are because the $^2\Pi$ states of CO are $n-\pi^*$ transitions, while the $^2\Pi$ states of N_2 are $\sigma-\pi^*$ transitions. The potential

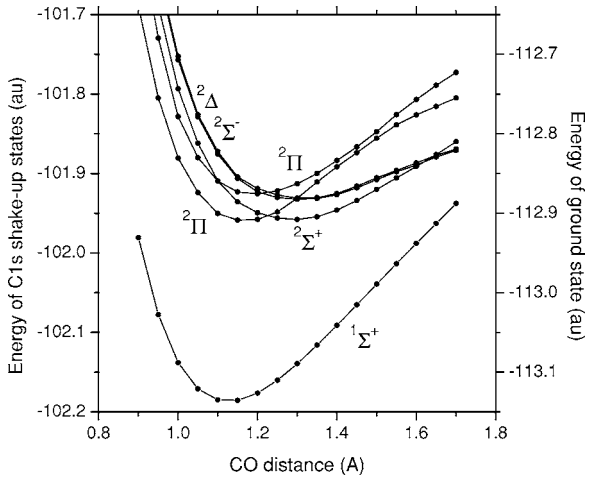

FIG. 3. Potential energy curves of the ground and C1*s* shake-up satellite states of CO calculated by the SAC-CI method

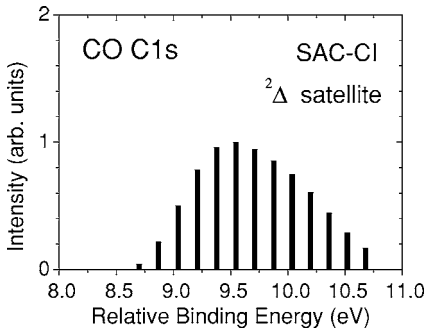

FIG. 5. The SAC-CI spectrum of C1*s* satellite $2\sigma^{-1}\pi^{-1}\pi^{*}$ $^2\Delta$ state.

energy curves of the $^2\Delta$ and $^2\Sigma^-$ states are almost parallel to those of the $^2\Sigma^+$ states. The $^2\Delta$ and $^2\Sigma^-$ states are nearly degenerate and their equilibrium distances are 1.309 and 1.320 Å for the $^2\Delta$ and $^2\Sigma^-$ states, respectively. These similarities are because all these states have the same $2\sigma^{-1}\pi^{-1}\pi^{*}$ character. The geometry relaxations for these $^2\Delta$ and $^2\Sigma^-$ states are 0.183 and 0.194 Å, respectively, which is also the same order as those of N_2, 0.192–0.194 Å.

To simulate the vibrationally resolved photoelectron spectrum, vibrational wave functions and FC factors were obtained by a numerical grid method. Thus, Fig. 4 compares the SAC-CI theoretical spectra obtained for the $^2\Sigma^+$ states to the experimental photoelectron satellite spectra. The experimental $^2\Sigma^+$ spectrum is approximated by $I(0)-cI(90)$, where $I(0)$ and $I(90)$ are spectral distributions of the 0° and 90° spectra, respectively, and c is the parameter that represents the contribution from the $^2\Pi$ component to the $I(0)$ spectrum. The parameter is set at $c=0.4$ so that the vibrational distribution of the Σ spectrum is close to the Poissonian. The theoretical spectrum is shifted in energy by −0.23 eV. The theoretical spectrum for $^2\Sigma^+$ has a maximum intensity at $v'=6$ and reproduces shape of the experimental spectrum. The activation of the high vibrational states is due to the large geometry relaxation. Deviations between the theoretical and experimental spectra in the higher vibrational states are due to errors in the calculated potential curves for large nuclear distances.

Figure 4 also compares the SAC-CI spectra for the $^2\Pi$ states to the experimental photoelectron satellite spectra recorded at 330 eV, where the 90° spectrum dominantly represents the Π component. The theoretical spectra are shifted in energy by −0.12 and −0.32 eV for the lower and higher $^2\Pi$ states, respectively. The relative intensities of the bands were adjusted so that the theoretical spectra agree with the experimental spectra: the vibrational intensity ratios are determined by the FC factors. The higher vibrational levels are less populated than those for N_2 because the $^2\Pi$ shake-up satellite states of CO are characterized as $n-\pi^{*}$ transitions, as noted above.

The theoretical spectrum for the $^2\Delta$ symmetry appears at higher energies and, as shown in Fig. 5, peaks at ~9.6 eV. The spectrum of the $^2\Sigma^-$ state is essentially the same as that of the $^2\Delta$ state. These states are located just above the present vibrational band and the experimental spectra show a

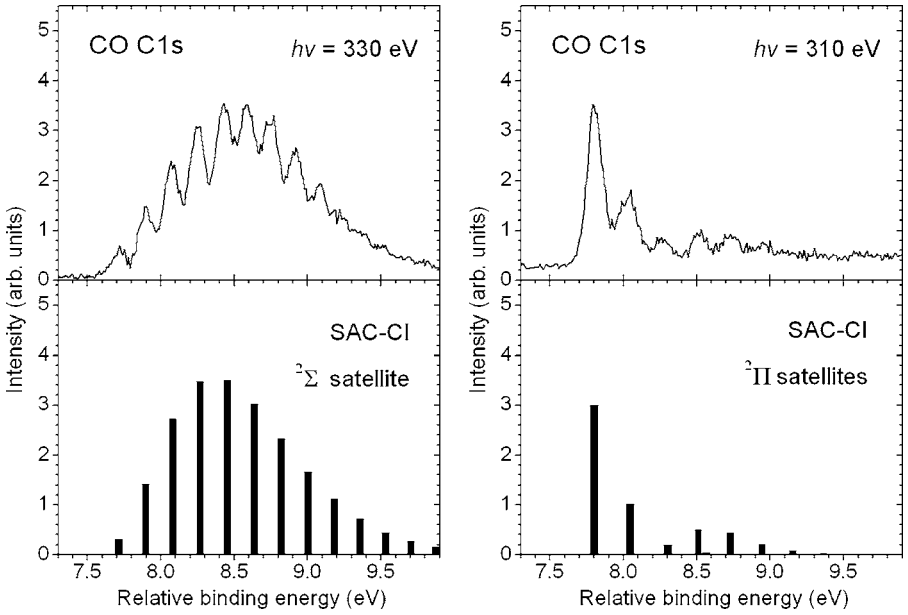

FIG. 4. Comparison between the photoelectron and SAC-CI spectra of the C1*s* satellite bands for $2\sigma^{-1}\pi^{-1}\pi^{*}$ $^2\Sigma^+$ (left) and $2\sigma^{-1}5\sigma^{-1}\pi^{*}$ $^2\Pi$ (right).

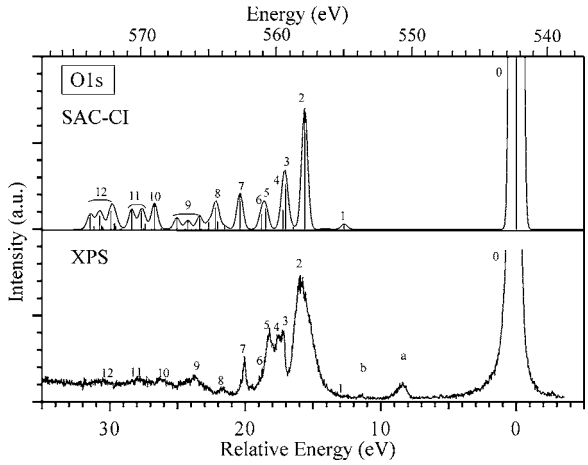

FIG. 6. O1*s* photoelectron satellite spectrum of CO. The experimental spectrum is recorded at a photon energy of 650 eV.

continuous shape in this energy region. The shape of the vibrational spectra of these states is very similar to that of the $^2\Sigma^+$ state due to the aforementioned reason.

C. O1*s* satellite spectrum

In contrast to the C1*s* spectrum of CO, which has been well studied by some theoretical methods[8–10] from the CI calculations by Guest *et al.*, theoretical analysis of the O1*s* satellite spectrum has been very limited. This satellite spectrum has significant orbital relaxation and electron correlations. Therefore, an accurate theoretical study requires the inclusion of the higher-order excitation operators. Actually, Angonoa *et al.* studied the low-energy region with ADC(4),[9] but their calculated spectrum differs from the experimental one. Fronzoni *et al.* performed the QDPTCI calculations and assigned a wide energy region up to ~28 eV.[10] In the present work, we measure the spectrum up to ~35 eV and perform the theoretical analysis with the SAC-CI method.

The present method calculates the O1*s* CEBE at 542.34 eV, in comparison with the recent experimental value of 542.543 eV.[40] Figure 6 compares the SAC-CI and XPS shake-up satellite spectra associated with the O1*s* ionization. The calculated and observed results of these shake-up states are summarized in Table III along with other works. As shown in Fig. 6, both the peak positions and relative intensities of the experimental satellite spectrum are reasonably reproduced by the SAC-CI calculation, even though both of the orbital relaxation and electron correlation effect are larger for the O1*s* ionization than for the C1*s* ionization.

Like formaldehyde, the O1*s* satellite spectrum should have different characteristics from the C1*s* spectrum.[22] The different features of these spectra can be interpreted in terms of charge transfer.[7] The lowest two satellites, peaks *a* and *b* in Fig. 6, are assigned to the conjugate satellites. The character of these satellites were previously studied by Schirmer *et al.*[12] The lowest monopole allowed peak 1, which is assigned to triplet $\pi^{-1}\pi^*$ transition, is calculated at 12.71 eV with a very small intensity of 0.0006. This state was also obtained by the QDPTCI at 13.76 eV.[10] The small structure is observed in the lower shoulder of peak 2 in the present XPS. Peak 2 is observed at 16.0 eV, which is the strongest with a relative intensity 0.065; this peak is calculated at 15.63 eV with an intensity of 0.014. The deviation in the intensity is large for this peak. Both bands 1 and 2 have significant contributions from a three-electron process $\pi^{-2}\pi^{*2}$ compared to the C1*s* ionization. Contrary to the C1*s* ionization, peak 2 does not have a vibrational structure, as discussed in Sec. IV D. In the QDPTCI calculation, two states at 15.90 and 16.14 eV with respective intensities of 0.006 and 0.079 are calculated for peak 2.[10]

Split bands 3 and 4 are observed near 17.2 eV. Two shake-up states, calculated at 17.05 and 17.24 eV, are attributed to these bands. These states are characterized as $5\sigma^{-1}\sigma^*$ transitions, which strongly interact with the three-electron processes of the $n^{-2}\pi^{*2}$ and $\pi^{-2}\pi^{*2}$ configurations. Band 5, which is observed at 18.23 eV, has a shoulder in the high energy region, and the corresponding shake-up states are $5\sigma^{-1}6\sigma$ transitions calculated at 18.51 and 18.80 eV. Sharp peak 7 is measured at 20.08 eV. For this band, we calculate the shake-up state at 20.40 eV with an intensity of 0.0043. This state is assigned to a $5\sigma^{-1}9\sigma$ transition.

In the region of 21.5–25 eV, broad continuous bands 8 and 9 are obtained at 21.65 and 23.83 eV, respectively. Many shake-up states for these bands are calculated at 21.55–25.05 eV; these states are dominantly assigned to the transition from the 5σ orbital to the Rydberg $n\sigma$ orbitals. Finally, in the energy region higher than ~26 eV, very broad bands 10–12 are observed. These broad bands are interpreted as the clusters of the shake-up states with small intensities calculated between 26.71 and 31.46 eV. These states are mainly characterized as Rydberg excitations from the 4σ orbital to the Rydberg $n\sigma$ orbitals accompanying the O1*s* ionization.

D. Low-lying O1*s* satellite states

Figure 7 presents the potential energy curves of the low-lying shake-up states of O1*s* ionization of CO. The two $^2\Sigma^+$ states, which are characterized as $1\sigma^{-1}\pi^{-1}\pi^*$, are calculated near 13.0 and 15.6 eV in vertical region and their potential curves are found to be repulsive. The lower $^2\Sigma^+$ state at ~13.0 eV has a contribution from a three electron process, $1\sigma^{-1}\pi^{-2}\pi^{*2}$, which explains the repulsive nature of the state. As noted in the previous section, the corresponding C1*s* shake-up state exists at much lower energy of ~8.4 eV. On the other hand, the higher singlet parent state exists at nearly the same energy of ~15.6 eV as the C1*s* ionization. In the energy region of 15–17 eV relative to the main line, two $^2\Delta$ and two $^2\Sigma^-$ states, which have the character of $1\sigma^{-1}\pi^{-1}\pi^*$, also exist as reported in ADC(4) work.[9] These states are also repulsive in nature and have almost the same transition character as the $^2\Sigma^+$ states. We have conducted high resolution measurement for the bands in this low-energy region. These bands do not show any vibrational structures, which confirm the repulsive nature predicted by the calculations.

The two shake-up satellite $^2\Pi$ states are obtained near ~5.1 and 8.8 eV in the Franck-Condon region. The vertical ionization energies of these states were also reported to be 5.03 and 8.7 eV by the ADC(4) calculations.[9] These two

TABLE III. Ionization energy (eV), relative energy to the main line (ΔE, eV), monopole intensity, and main configurations of the O1*s* satellite states of CO.

Other							This work						
Expt.[a]		Expt.[b]		ADC(4)[c]		QDPTCI[d]	Expt.		SAC-CI general *R*				
ΔE	Int.	ΔE	Int.	ΔE	Int.	ΔE	ΔE	Int.	No.	IP	ΔE	Int.	Main configurations ($\|C\|>0.3$)
542.57[e]	1			541.56	1	541.76	0	1	0	542.34	0.00	1	$0.83(1\sigma^{-1})-0.24(\pi^{-1}\pi^{*}1\sigma^{-1})-0.24(\pi^{-1}\pi^{*}1\sigma^{-1})$
		8.5	0.005			13.76			1	555.05	12.71	0.0006	$0.60(1\sigma^{-1}\pi^{*}\pi^{-1})+0.60(1\sigma^{-1}\pi^{*}\pi^{-1})$
		11.5	0.004										$-0.24(\pi^{-1}\pi^{*}1\sigma^{-1}\pi^{*}\pi^{-1})-0.24(\pi^{-1}\pi^{*}1\sigma^{-1}\pi^{*}\pi^{-1})$
15.9	0.112	16	0.065	17.00	0.004	15.90, 16.14	16.00	0.065	2	557.97	15.63	0.0143	$0.47(\pi^{-1}\pi^{*}1\sigma^{-1})+0.47(\pi^{-1}\pi^{*}1\sigma^{-1})$
													$+0.24(5\sigma^{-1}\sigma^{*}1\sigma^{-1})+0.43(\pi^{-1}\pi^{*}1\sigma^{-1}\pi^{*}\pi^{-1})$
17.25	0.013	17.5	0.031	17.47	0.002	16.83	17.28	0.026	3	559.39	17.05	0.0053	$0.48(1\sigma^{-1}\sigma^{*}5\sigma^{-1})+0.46(5\sigma^{-1}\sigma^{*}1\sigma^{-1})$
													$-0.41(5\sigma^{-1}\pi^{*}5\sigma^{-1}\pi^{*}1\sigma^{-1})-0.41(\pi^{-1}\pi^{*}\pi^{-1}\pi^{*}1\sigma^{-1})$
						17.65			4	559.58	17.24	0.0023	$0.58(1\sigma^{-1}\sigma^{*}5\sigma^{-1})+0.28(1\sigma^{-1}6\sigma5\sigma^{-1})$
													$+0.35(5\sigma^{-1}\pi^{*}5\sigma^{-1}\pi^{*}1\sigma^{-1})+0.35(5\sigma^{-1}\pi^{*}5\sigma^{-1}\pi^{*}1\sigma^{-1})$
18.11	0.042	18.3	0.032	18.37	0.009	18.41	18.23	0.020	5	560.85	18.51	0.0024	$0.47(1\sigma^{-1}6\sigma5\sigma^{-1})+0.42(1\sigma^{-1}9\sigma5\sigma^{-1})+0.36(1\sigma^{-1}7\sigma5\sigma^{-1})$
													$-0.30(1\sigma^{-1}\sigma^{*}5\sigma^{-1})-0.29(5\sigma^{-1}\sigma^{*}1\sigma^{-1})$
									6	561.14	18.80	0.0017	$0.67(5\sigma^{-1}6\sigma1\sigma^{-1})+0.40(5\sigma^{-1}9\sigma1\sigma^{-1})$
													$+0.27(5\sigma^{-1}7\sigma1\sigma^{-1})+0.23(1\sigma^{-1}6\sigma5\sigma^{-1})$
20.06	0.012	20.2	0.014	20.32	0.015	19.70, 20.18	20.08	0.009	7	562.74	20.40	0.0043	$0.54(5\sigma^{-1}9\sigma1\sigma^{-1})-0.27(5\sigma^{-1}\sigma^{*}1\sigma^{-1})-0.26(5\sigma^{-1}7\sigma1\sigma^{-1})$
				20.54	0.015								
21.7		21.6	0.006	21.67	0.059	21.25, 21.79	21.65	0.004	8	563.89	21.55	0.0004	$0.52(1\sigma^{-1}10\sigma5\sigma^{-1})+0.47(1\sigma^{-1}7\sigma5\sigma^{-1})+0.36(\sigma^{-1}11\sigma5\sigma^{-1})$
				22.11	0.006					564.41	22.07	0.0009	$0.71(1\sigma^{-1}9\sigma5\sigma^{-1})-0.33(1\sigma^{-1}6\sigma5\sigma^{-1})$
										564.54	22.20	0.0025	$0.46(5\sigma^{-1}11\sigma1\sigma^{-1})+0.44(5\sigma^{-1}7\sigma1\sigma^{-1})+0.37(5\sigma^{-1}10\sigma1\sigma^{-1})$
													$-0.35(5\sigma^{-1}6\sigma1\sigma^{-1})+0.29(5\sigma^{-1}7\sigma1\sigma^{-1})$
										565.04	22.70	0.0009	$0.76(5\sigma^{-1}9\sigma1\sigma^{-1})-0.32(5\sigma^{-1}6\sigma1\sigma^{-1})-0.28(5\sigma^{-1}7\sigma1\sigma^{-1})$
													$+0.27(1\sigma^{-1}9\sigma5\sigma^{-1})$
23.7		23.6	0.014	22.5	0.043	23.12, 23.56	23.83	0.012	9	565.72	23.38	0.0015	$0.61(5\sigma^{-1}11\sigma1\sigma^{-1})-0.44(1\sigma^{-1}10\sigma5\sigma^{-1})$
				24.19	0	24.01, 24.64				566.59	24.25	0.0011	$0.80(5\sigma^{-1}10\sigma1\sigma^{-1})+0.34(1\sigma^{-1}10\sigma5\sigma^{-1})$
						25.00, 25.27				567.39	25.05	0.0014	$0.53(5\sigma^{-1}\pi^{*}4\sigma^{-1}\pi^{*}1\sigma^{-1})+0.53(5\sigma^{-1}\pi^{*}4\sigma^{-1}\pi^{*}1\sigma^{-1})$
						25.41							$+0.35(4\sigma^{-1}\pi^{*}1\sigma^{-1}\pi^{*}5\sigma^{-1})+0.34(4\sigma^{-1}\pi^{*}1\sigma^{-1}\pi^{*}5\sigma^{-1})$
26.2		26.4	0.011			26.52, 26.76	26.37	0.011	10	569.05	26.71	0.0031	$0.39(1\sigma^{-1}6\sigma4\sigma^{-1})-0.27(4\sigma^{-1}6\sigma1\sigma^{-1})$
													$-0.23(4\sigma^{-1}\pi^{*}1\sigma^{-1}\pi^{*}5\sigma^{-1})$
27.9		27.8	0.012			27.57, 27.80	27.98	0.012	11	570.01	27.67	0.0021	$0.39(1\sigma^{-1}7\sigma1\sigma^{-1})-0.34(\pi^{-1}3\pi1\sigma^{-1})$
						27.96, 28.55				570.72	28.38	0.0024	$0.38(1\sigma^{-1}7\sigma1\sigma^{-1})-0.33(\pi^{-1}3\pi1\sigma^{-1})$
~31		30.7	0.011				30.73	0.011	12	572.27	29.93	0.0021	$0.35(1\sigma^{-1}3\pi\pi^{-1})+0.27(1\sigma^{-1}4\pi\pi^{-1})$
										573.12	30.78	0.0016	$0.69(1\sigma^{-1}3\pi\pi^{-1})+0.49(\pi^{-1}3\pi1\sigma^{-1})$
										573.80	31.46	0.0017	$0.33(\pi^{-1}3\pi\sigma^{-1})+0.29(5\sigma^{-1}3\pi1\sigma^{-1})+0.29(1\sigma^{-1}7\sigma5\sigma^{-1})$

[a]Reference 6.
[b]Reference 7.
[c]Reference 9.
[d]Reference 10.
[e]Reference 40.

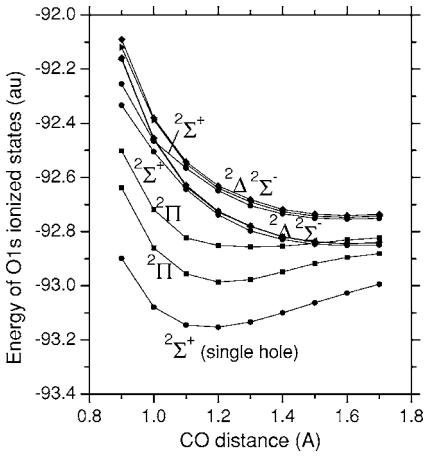

FIG. 7. Potential energy curves of the O1*s* shake-up satellite states of CO calculated by the SAC-CI method.

states are characterized as $1\sigma^{-1}n^{-1}\pi^*$ with a small contribution from the three electron processes. The lower $^2\Pi$ state is calculated to be deeply bound and its spectroscopic constants are $R_e=1.221$ Å, $\omega_e=1957$ cm^{-1}, and $\omega_e\chi_e=14.5$ cm^{-1}. However, the Franck-Condon region of this state is near the threshold of the dissociation limit in energy. Thus, the vibrational structure should not be observed. The same is true for the higher $^2\Pi$ state. This state is much more weakly bound and its potential energy curve is almost flat. As shown in Fig. 6, the lower $^2\Pi$ state is not detected in the XPS spectrum, and the higher $^2\Pi$ state has a very small intensity as expected in high energy excitation of the conjugate shake-up satellites.

V. SUMMARY

The C1*s* and O1*s* satellite spectra of CO have been measured using high-resolution x-ray photoelectron spectroscopy; numerous new peaks are resolved in the present spectra. Detailed analyses of the spectra have been performed with the SAC-CI general-*R* method. The general-*R* method, which includes triple and quadruple *R* operators, has well reproduced the satellite bands of the inner-shell photoelectron spectra of CO, whose orbital reorganizations and electron correlations have been recognized as to be large in the previous theoretical works.

From theoretical and experimental analysis, 16 and 12 bands have been identified in the C1*s* and O1*s* satellite spectra of CO up to about ~32 eV relative to the main lines. Detailed assignments have been provided for these bands and some of them are new interpretations. The satellite peaks above the $\pi^{-1}\pi^*$ transitions are mainly attributed to the Rydberg excitations that accompany the core ionizations. Many shake-up states which strongly interact with three-electron processes such as $\pi^{-2}\pi^{*2}$ and $n^{-2}\pi^{*2}$, have been calculated in the low-energy region. In the higher-energy region, continuous Rydberg excitations have been calculated with small intensities, which contrasts the inner-shell satellite spectra of formaldehyde.[22]

For the low-lying C1*s* satellite bands, we have executed the vibrational analysis. *Ab initio* analysis is well correlated to the experimental data, namely, one $^2\Sigma^+$ state and two $^2\Pi$ shake-up states are confirmed to be attributed to the vibrational structures observed in the experimental spectra; the shake-up $^2\Delta$ and $^2\Sigma^-$ states are predicted to be above the vibrational bands. This excellent agreement confirms the reliability of the present *ab initio* potential curves of these shake-up satellite states. For the O1*s* shake-up states, the potential curves have been calculated to be weakly bound or repulsive.

ACKNOWLEDGMENTS

This study has been supported by a Grant for Creative Scientific Research from the Ministry of Education, Science, Culture, and Sports of Japan and by Grants-in-Aid for Scientific Research from the Japanese Society for the Promotion of Science. This experiment was conducted with the approval of the SPring-8 program advisory committee. We are grateful to the staff at SPring-8 for their help.

[1] L. S. Cederbaum, W. Domcke, J. Schirmer, and W. von Niessen, Adv. Chem. Phys. **65**, 115 (1986).
[2] K. Ueda, J. Phys. B **36**, R1 (2003).
[3] U. Hergenhahn, J. Phys. B **37**, R89 (2004); K. J. Borve, L. J. Saethre, T. D. Thomas, T. X. Carroll, N. Berrah, J. D. Bozek, and E. Kukk, Phys. Rev. A **63**, 012506 (2001); T. Karlsen, L. J. Saethre, K. J. Borve, N. Berrah, J. D. Bozek, T. X. Carroll, and T. D. Thomas, J. Phys. Chem. A **105**, 7700 (2001).
[4] K. Siegbahn, C. Nordling, G. Johansson *et al.*, *ESCA Applied to Free Molecules* (North-Holland, Amsterdam, 1969).
[5] U. Gelius, J. Electron Spectrosc. Relat. Phenom. **5**, 985 (1974).
[6] J. Schirmer, G. Angonoa, S. Svensson, D. Nordfors, and U. Gelius, J. Phys. B **20**, 6031 (1987).
[7] D. Nordfors, A. Nilsson, N. Martensson, S. Svensson, U. Gelius, and H. Agren, J. Electron Spectrosc. Relat. Phenom. **56**, 117 (1991).
[8] M. F. Guest, W. R. Rodwell, T. Darko, I. H. Hillier, and J. Kendrick, J. Chem. Phys. **66**, 5447 (1977).
[9] G. Angonoa, I. Walter, and J. Schirmer, J. Chem. Phys. **87**, 6789 (1987).
[10] G. Fronzoni, G. D. Alti, and P. Decleva, J. Phys. B **32**, 5357 (1999).
[11] A. Thiel, J. Schirmer, and H. Köppel, J. Chem. Phys. **119**, 2088 (2003).
[12] J. Schirmer, M. Braunstein, and V. McKoy, Phys. Rev. A **41**, 283 (1990).
[13] M. Matsumoto, K. Ueda, E. Kukk *et al.*, Chem. Phys. Lett. **417**, 89 (2006).
[14] M. Ehara, H. Nakatsuji, M. Matsumoto *et al.*, J. Chem. Phys. **124**, 124311 (2006).
[15] H. Nakatsuji, Chem. Phys. Lett. **59**, 362 (1978); **67**, 329 (1979).
[16] K. Ueda, M. Hoshino, T. Tanaka *et al.*, Phys. Rev. Lett. **94**, 243004 (2005).
[17] H. Nakatsuji, Chem. Phys. Lett. **177**, 331 (1991); J. Chem. Phys. **83**, 713 (1985).
[18] M. Ehara and H. Nakatsuji, Chem. Phys. Lett. **282**, 347 (1998); M. Ehara, M. Ishida, K. Toyota, and H. Nakatsuji, *Reviews in Mordern Quantum Chemistry* (World Scientific, Singapore 2002); M. Ehara, J. Hasegawa, and H. Nakatsuji, *SAC-CI Method Applied to Molecular Spectroscopy, in Theory and Applications of Computational Chemistry: The First* 40 Years*, A Volume of Technical and Historical Perspectives* (Elsevier, New York, 2005).
[19] K. Kuramoto, M. Ehara, and H. Nakatsuji, J. Chem. Phys. **122**, 014304 (2005).
[20] R. Sankari, M. Ehara, H. Nakatsuji, Y. Senba, K. Hosokawa, H. Yoshida, A. D. Fanis, Y. Tamenori, S. Aksela, and K. Ueda, Chem. Phys. Lett. **380**, 647 (2003).
[21] R. Sankari, M. Ehara, H. Nakatsuji, A. D. Fanis, S. Aksela, S. L. Sorensen, M. N. Piancastelli, and K. Ueda, Chem. Phys. Lett. **422**, 51 (2006).
[22] K. Kuramoto, M. Ehara, H. Nakatsuji, M. Kitajima, H. Tanaka, A. D. Fanis, Y. Tamenori, and K. Ueda, J. Electron Spectrosc. Relat. Phenom. **142**, 253 (2005).
[23] H. Ohashi, E. Ishiguro, Y. Temanori, H. Kishimoto, M. Tanaka, M. Irie, and T. Ishikawa, Nucl. Instrum. Methods Phys. Res. A **467–468**, 529 (2001).
[24] K. Ueda, H. Yoshida, Y. Senba *et al.*, Nucl. Instrum. Methods Phys. Res.

A **467–468**, 1502 (2001); Y. Tamenori, H. Ohashi, E. Ishiguro, and T. Ishikawa, Rev. Sci. Instrum. **73**, 1588 (2002).
[25] T. Tanaka and H. Kitamura, J. Synchrotron Radiat. **3**, 47 (1996).
[26] Y. Shimizu, H. Ohashi, Y. Tamenori *et al.*, J. Electron Spectrosc. Relat. Phenom. **114–116**, 63 (2001).
[27] D. A. Mistrov, A. D. Fanis, M. Kitajima, M. Hoshino, H. Shindo, T. Tanaka, Y. Tamenori, H. Tanaka, A. A. Pavlychev, and K. Ueda, Phys. Rev. A **68**, 022508 (2003); M. Hoshino, T. Tanaka, M. Kitajima, H. Tanaka, A. D. Fanis, A. A. Pavlychev, and K. Ueda, J. Phys. B **36**, L381 (2003).
[28] J. H. Callomon, E. Hirota, K. Kuchitsu, W. J. Lafferty, A. G. Maki, and C. S. Pote, *Structure Data of Free Polyatomic Molecules*, Numerical Data and Functional Relationships in Science and Technology Landolt-Bornstein, New Series, Group II (Springer-Verlag, Berlin, 1976).
[29] A. Schaefer, C. Huber, and R. Ahlrichs, J. Chem. Phys. **100**, 5829 (1994).
[30] T. H. Dunning, Jr., J. Chem. Phys. **90**, 1007 (1989).
[31] T. H. Dunning, Jr. and P. J. Hay, *Methods of Electronic Structure Theory* (Plenum, New York, 1977).
[32] H. Nakatsuji, Chem. Phys. **75**, 425 (1983).
[33] R. I. Martin and D. A. Shirley, J. Chem. Phys. **64**, 3685 (1976).
[34] M. J. Frisch, G. W. Trucks, H. B. Schlegel *et al.*, GAUSSIAN03, Gaussian Inc., Pittsburgh, PA, 2003.
[35] G. A. Worth, M. H. Beck, A. Jackle, and H.-D. Meyer, The MCTDH Package, Version 8.3, University Heidelberg, Heidelberg, Germany, 2003.
[36] V. Myrseth, J. D. Bozek, E. Kukk, L. J. Sæthre, and T. D. Thomas, J. Electron Spectrosc. Relat. Phenom. **122**, 57 (2002).
[37] A. D. O. Bawagan and E. R. Davidson, Adv. Chem. Phys. **110**, 215 (1999).
[38] U. Becker and D. A. Shirley, Phys. Scr., T **T31**, 56 (1990).
[39] L. Ungier and T. D. Thomas, Phys. Rev. Lett. **53**, 435 (1984).
[40] R. Püttner, I. Dominguez, T. J. Morgan, C. Cisneros, R. F. Fink, E. Rotenberg, T. Warwick, M. Comke, G. Kaindl, and A. S. Schlachter, Phys. Rev. A **59**, 3415 (1999).